# RESPONSE OF NONLINEAR PANELS TO RANDOM LOADS*

Chuh Mei
Old Dominion University

## SUMMARY

Lightweight aircraft structures exposed to a high intensity noise environ-
ment can fatigue fail prematurely if adequate consideration is not given to the
problem. Design methods and design criteria for sonic fatigue prevention have
been developed based on analytical and experimental techniques. Most of the
analytical work was based upon small deflection or linear structural theory
which did not agree with the experimental results. A large deflection geomet-
rical nonlinearity was incorporated into the analysis methods for determining
the structural response to high intensity noise. The Karman-Herrmann large
deflection equations with a single-mode Galerkin approximation, and the method
of equivalent linearization were used to predict mean-square amplitude, mean-
square stresses, and nonlinear frequency at various acoustic loadings for
rectangular panels. Both simply supported and clamped support conditions with
immovable or movable inplane edges are considered. Comparisons with experimen-
tal results are presented.

## INTRODUCTION

Vibrations caused by acoustic pressure can frequently disturb the operating
conditions of various instruments and systems, and sonic fatigue failures which
occurred in aircraft structural components cause large maintenance and inspec-
tion burdens. The development of sonic fatigue data and design techniques were
initiated to prevent sonic fatigue failures. Design methods and design criteria
for many types of aircraft structures have been developed under Air Force
sponsorship and by the industry in the past twenty years. Reference 1 has a
complete list of the reports describing these efforts. This research led to
sonic fatigue design criteria and design charts which are widely used during
the design of an aircraft. Although current analytical sonic fatigue design
methods are essentially based on small deflection or linear structural theory
(see ref. 1, page 209), many documented tests (refs. 2 - 6) on various aircraft
panels have indicated that high noise levels in excess of 110 decibels (dB)
produce nonlinear behavior with large amplitudes of one to two times the

panel thickness in such structural panels. The neglect of such large deflection geometrical nonlinearity in analysis and design formulations has been identified as one of the major causes for poor agreement between experimental data and analytical results. The evidence of those researchers was summarized in reference 7, where a comprehensive review of existing analytical methods on random excitations of nonlinear systems was also given.

In this paper, the Karman-Herrmann large deflection equations for rectangular plates (ref. 8) are employed. Using a single-mode Galerkin's approximation, the dynamic equations reduce to a nonlinear differential equation with time as the independent variable. The method of equivalent linearization (refs. 9 - 11) is then applied to reduce the nonlinear equation to an equivalent linear one. Mean-square displacements, mean-square stresses, and nonlinear frequencies at various acoustic loadings are obtained for rectangular panels of different aspect ratios and damping factors. Both simply supported and clamped boundary conditions with immovable or movable inplane edges are considered. Comparisons with experimental results are also presented.

## SYMBOLS

| | |
|---|---|
| $a,b$ | Panel length and width |
| $A,B$ | Panel dimension parameters, $2\pi/a$ and $2\pi/b$ |
| $C_1, C_2$ | Constants |
| $D$ | Bending rigidity |
| $err$ | Error of linearization |
| $E$ | Young's modulus |
| $f$ | Equivalent linear frequency in Hz |
| $F$ | Stress function |
| $h$ | Panel thickness |
| $H(\omega)$ | Frequency response function |
| $L$ | Spectrum level |
| $m$ | Mass coefficient |
| $N$ | Membrane stress resultant |
| $\bar{N}$ | Constant |
| $p$ | Pressure loading |
| $q$ | Generalized or modal displacement |
| $r$ | Aspect ratio, $a/b$ |
| $S(\omega)$ | Spectral density function of excitation pressure $p(t)$ |
| $t$ | Time |
| $u,v$ | Displacement of midplane |
| $w$ | Transverse deflection |
| $x,y,z$ | Coordinates |
| $\beta$ | Nonlinearity coefficient |
| $\beta*$ | Nondimensional nonlinearity coefficient |
| $\zeta$ | Ratio of damping to critical damping |
| $\lambda$ | Nondimensional frequency parameter |
| $\nu$ | Poisson's ratio |
| $\rho$ | Panel mass density |
| $\sigma, \tau$ | Normal and shear stresses |

ω        Radian frequency
Ω        Equivalent linear or nonlinear radian frequency
Subscripts:
b        Bending
c        Complementary solution or critical
m        Membrane
max      Maximum
o        Linear
p        Particular solution

## FORMULATION AND SOLUTION PROCEDURE

### Governing Equations

Assuming that the effect of both the inplane and rotatory inertia forces can be neglected, the dynamic von Karman equations of a rectangular isotropic plate undergoing moderately large deflections are (refs. 8, 12):

$$L(w,F) = D\nabla^4 w + \rho h w_{,tt} - h\,(F_{,yy}\,w_{,xx} + F_{,xx}\,w_{,yy}$$

$$-2F_{,xy}\,w_{,xy}) - p(t) = 0 \tag{1}$$

$$\nabla^4 F = E\,(w^2_{,xy} - w_{,xx}\,w_{,yy}) \tag{2}$$

where w is the transverse deflection of the plate, h is the panel thickness, $\rho$ is the mass density of the panel material, $D = Eh^3/12(1-\nu^2)$ is the flexural rigidity, E is Young's modulus, $\nu$ is Poisson's ratio, p(t) is the exciting pressure, and a comma preceding a subscript(s) indicates partial differentiation (s). The stress function F is defined by

$$\sigma_x = F_{,yy}$$

$$\sigma_y = F_{,xx} \tag{3}$$

$$\tau_{xy} = -F_{,xy}$$

where $\sigma_x$, $\sigma_y$, and $\tau_{xy}$ are membrane stresses.

Simply Supported Panels. For a rectangular plate simply supported along all four edges as shown in Figure 1, Chu and Herrmann (ref. 8), and Lin (ref. 13) have considered that if the fundamental mode is predominant, the motion of the panel can be represented adequately as

$$w = q(t)\,h \cos(\pi x/a) \cos(\pi y/b) \tag{4}$$

where q(t) is a function of time only. The maximum value of q(t) coincides with

the maximum deflection $w_{max}$ divided by panel thickness h. The expression w satisfies the boundary conditions for simple supports

$$w = w,_{xx} + \nu\, w,_{yy} = 0, \text{ on } x = \pm\, a/2$$

$$w = w,_{yy} + \nu\, w,_{xx} = 0, \text{ on } y = \pm\, b/2 \tag{5}$$

Substituting the expression for w in Eq. (2) and solving for a particular solution $F_p$ yields

$$F_p = -\frac{1}{32}\, q^2 h^2 E r^2 \left( \cos\frac{2\pi x}{a} + \frac{1}{r^4}\cos\frac{2\pi y}{b} \right) \tag{6}$$

where $r = a/b$. The complementary solution to equation (2) is taken in the form

$$F_c = \overline{N}_x\, \frac{y^2}{2} + \overline{N}_y\, \frac{x^2}{2} \tag{7}$$

where the constants $\overline{N}_x$ and $\overline{N}_y$ contribute to the membrane stresses $\sigma_x$ and $\sigma_y$ and are to be determined from the inplane boundary, immovable or movable, conditions.

For the immovable edges case, the conditions of zero inplane normal displacement at all four edges are satisfied in an averaged manner as

$$\iint \frac{\partial u}{\partial x}\, dxdy = \iint \left[ \frac{1}{E}\, (F,_{yy} - \nu F,_{xx}) - \tfrac{1}{2}\, w^2,_x \right] dxdy, \text{ on } x = \pm\, a/2$$

$$\iint \frac{\partial v}{\partial y}\, dydx = \iint \left[ \frac{1}{E}\, (F,_{xx} - \nu F,_{yy}) - \tfrac{1}{2}\, w^2,_y \right] dydx, \text{ on } y = \pm\, b/2 \tag{8}$$

where u and v are inplane displacements. For the movable edges case, the edges are free to move as a rigid body with the average inplane stress equal to zero. The inplane boundary conditions are

$$\left. \begin{array}{l} N_x = h \displaystyle\int_{-b/2}^{b/2} F,_{yy}\, dy = 0 \\[12pt] u = \text{constant} \end{array} \right\}, \qquad \text{on } x = \pm\, a/2$$

$$\left. \begin{array}{l} N_y = h \displaystyle\int_{-a/2}^{a/2} F,_{yy}\, dx = 0 \\[12pt] v = \text{constant} \end{array} \right\}, \qquad \text{on } y = \pm\, b/2 \tag{9}$$

where $N_x$ and $N_y$ are membrane stress resultants per unit length in plate. By

making use of these inplane edge boundary conditions, equations (8) and (9), it easily can be shown that for the immovable edges

$$\overline{N}_x = \frac{q^2 h^2 E \pi^2}{8a^2 (1-\nu^2)} (1 + \nu r^2)$$

$$\overline{N}_y = \frac{q^2 h^2 E \pi^2}{8a^2 (1-\nu^2)} (r^2 + \nu) \tag{10}$$

and for the movable edges

$$\overline{N}_x = \overline{N}_y = 0 \tag{11}$$

the complete stress function is then given by $F = F_p + F_c$.

With the assumed w given by equation (4) and stress function given by equations (6) and (7), equation (1) is satisfied by applying Galerkin's method

$$\int_{-a/2}^{a/2} \int_{-b/2}^{b/2} L(w,F) \, w \, dxdy = 0 \tag{12}$$

from which yields the modal equation of the form

$$\ddot{q} + \omega_o^2 q + \beta q^3 = \frac{p(t)}{m} \tag{13}$$

and

$$\omega_o^2 = \lambda_o^2 \frac{D}{\rho h b^4}, \quad \lambda_o^2 = \pi^4 (1 + \frac{1}{r^2})^2$$

$$m = \pi^2 \rho h^2 / 16 \tag{14}$$

$$\beta = \beta_p + \beta_c = (\beta_p^* + \beta_c^*) \frac{D}{\rho h b^4}$$

with

$$\beta_p^* = \frac{3\pi^4}{4r^4} (1 + r^4)(1 - \nu^2)$$

$$\beta_c^* = \frac{3\pi^4}{2r^4} (1 + 2\nu r^2 + r^4)$$

where $\omega_o$ is linear radian frequency, m is mass coefficient, and $\beta$ is nonlinearity coefficient. The linear frequency $\lambda_o$, nonlinearity coefficients $\beta_p^*$ and $\beta_c^*$, and aspect ratio r are all nondimensional parameters.

<u>Clamped Panels.</u>  Yamaki (ref. 14) considered the predominant mode

$$w = \frac{q(t)h}{4} \left(1 + \cos \frac{2\pi x}{a}\right)\left(1 + \cos \frac{2\pi y}{b}\right) \tag{15}$$

which satisfies the clamped support conditions

$$w = w_{,x} = 0, \qquad \text{on } x = \pm a/2$$

$$w = w_{,y} = 0, \qquad \text{on } y = \pm b/2 \tag{16}$$

By introducing equation (15) in equation (2) and solving it, the particular stress function is

$$F_p = -\frac{1}{32} q^2 h^2 E r^2 \left[\cos Ax + \frac{1}{r^4}\cos By + \frac{1}{16}\cos 2Ax\right.$$

$$+ \frac{2}{(1+r^2)^2}\cos Ax \cos By + \frac{1}{16r^4}\cos 2By$$

$$\left.+ \frac{1}{(4+r^2)^2}\cos 2Ax \cos By + \frac{1}{(1+4r^2)^2}\cos Ax \cos 2By\right] \tag{17}$$

where  $A = 2\pi/a$  and  $B = 2\pi/b$.  The complementary stress function is assumed as the form appearing in equation (7).  Upon enforcing the inplane edge conditions, equations (8) and (9), it can be shown that for the immovable edges

$$\bar{N}_x = \frac{3q^2 h^2 E \pi^2}{32\, a^2(1-\nu^2)}(1+\nu r^2)$$

$$\bar{N}_y = \frac{3q^2 h^2 E \pi^2}{32\, a^2(1-\nu^2)}(r^2+\nu) \tag{18}$$

and for the movable edges

$$\bar{N}_x = \bar{N}_y = 0 \tag{19}$$

the complete stress function is given by $F = F_p + F_c$.  Introducing these expressions for w and F in equation (1) and applying Galerkin's procedure yields the equation

$$\ddot{q} + \omega_o^2\, q + \beta q^3 = \frac{p(t)}{m} \tag{13}$$

where

$$\omega_o^2 = \lambda_o^2 \frac{D}{\rho h b^4}, \qquad \lambda_o^2 = \frac{16\pi^4}{9r^4} (3 + 2r^2 + 3r^4)$$

$$m = 9 \rho h^2/16 \tag{20}$$

$$\beta = \beta_p + \beta_c = (\beta_p^* + \beta_c^*) \frac{D}{\rho h b^4}$$

and

$$\beta_p^* = \frac{4}{3} \pi^4 (1-\nu^2) \left[1 + \frac{1}{r^4} + \frac{1}{16} + \frac{2}{(1 + r^2)^2} + \frac{1}{16r^4}\right.$$

$$\left. + \frac{1}{2(4 + r^2)^2} + \frac{1}{2(1 + 4r^2)^2}\right] \tag{21}$$

$$\beta_c^* = \frac{3\pi^4}{2r^4} (1 + 2\nu r^2 + r^4)$$

Equation (13) represents the undamped, large-amplitude vibration of a rectangular panel with simply supported or damped edges.

The methods commonly used for determining the damping coefficient are the bandwidth method in which half-power widths are measured at modal resonances, and the decay rate method in which the logarithmic decrement of decaying modal response traces is measured. The values of damping ratio $\zeta$ range from 0.005 to 0.05 for the common type of panel construction used in aircraft structures. Once the damping coefficient is determined from experiments or from existing data of similar construction, the modal equation, equation (13), now reads

$$\ddot{q} + 2\zeta\omega_o\dot{q} + \omega_o^2 q + \beta q^3 = \frac{p(t)}{m} \tag{22}$$

The method of equivalent linearization is then employed to determine an approximate root-mean-square (RMS) displacement from equation (22).

## Method of Equivalent Linearization

The basic idea of the equivalent linearization (refs. 9 - 11) is to replace the original nonlinear equation, equation (22), with an equation of the form

$$\ddot{q} + 2\zeta\omega_o\dot{q} + \Omega^2 q + err\ (q) = \frac{p(t)}{m} \tag{23}$$

where $\Omega$ is an equivalent linear or nonlinear frequency, and err is the error of linearization. An equivalent linear equation is obtained by omitting this error term, then equation (23) is linear and it can be readily solved. The error of linearization is

$$err = (\omega_0^2 - \Omega^2)\, q + \beta q^3 \tag{24}$$

which is the difference between equation (22) and equation (23). The smaller that the error is, the smaller the error in neglecting it, and the better approximate solution to equation (22) will be obtained. To this end, the equivalent linear frequency square $\Omega^2$ in the linearized equation is chosen in such a way that the mean-square error $err^2$ is minimized, that is

$$\frac{\partial (err^2)}{\partial (\Omega^2)} = 0 \tag{25}$$

If the acoustic pressure excitation p(t) is stationary Gaussian and ergodic, then the response q computed from the linearized equation, equation (23), must also be Gaussian. Substituting equation (24) into equation (25) yields (refs. 9, 13)

$$\Omega^2 = \omega_0^2 + 3\beta \overline{q^2} \tag{26}$$

where $\overline{q^2}$ is the maximum mean-square deflection of the panel. Dividing both sides of equation (26) by $D/\rho h b^4$ yields

$$\lambda^2 = \lambda_0^2 + 3\beta^* \overline{q^2} \tag{27}$$

where $\lambda^2$ is a nondimensional equivalent linear or nonlinear frequency parameter.

An approximate solution of equation (23) is obtained by dropping the error term; the mean-square response of amplitude is

$$\overline{q^2} = \int_0^\infty S(\omega)\, |H(\omega)|^2\, d\omega \tag{28}$$

where $S(\omega)$ is the spectral density function of the excitation pressure $\dot{p}(t)$, and the frequency response function $H(\omega)$ is given by

$$H(\omega) = \frac{1}{m(\Omega^2 - \omega^2 + 2i\zeta\omega_0\omega)} \tag{29}$$

For lightly damped ($\zeta \leq 0.05$) structures, the response curves will be highly peaked at $\Omega$. The integration of equation (28) can be greatly simplified if the forcing spectral density function $S(\omega)$ can be considered to be constant in the frequency band surrounding the nonlinear resonance peak $\Omega$, so that

$$\overline{q^2} \simeq \frac{\pi S(\Omega)}{4m^2 \zeta \omega_o \Omega^2} \tag{30}$$

In practice, the spectral density function is generally given in terms of the frequency f in Hertz. To convert the previous result one must substitute

$$\Omega = 2\pi f \tag{31}$$

and $\quad S(\Omega) = S(f)/2\pi$

into equation (30); the mean-square peak deflection is simply

$$\overline{q^2} = \begin{cases} \dfrac{32 \, S_f}{\pi^4 \zeta \lambda_o \lambda^2} & , \quad \text{for simply supported panels} \\[4mm] \dfrac{32 \, S_f}{81 \zeta \lambda_o \lambda^2} & , \quad \text{for clamped panels} \end{cases} \tag{32}$$

The pressure spectral density function $S(f)/2\pi$ has the units $(Pa)^2/Hz$ or $(psi)^2/Hz$, and $S_f$ is a nondimensional forcing excitation spectral density parameter defined as

$$S_f = \frac{S(f)}{\rho^2 h^4 (D/\rho h b^4)^{3/2}} \tag{33}$$

The linear frequency parameters $\lambda_o$ in equations (32) are given in equation (14) and equation (20) for simply supported and clamped panels, respectively, and the equivalent frequency parameters $\lambda^2$ can be determined through equation (27).


### Solution Procedure

The mean-square response $\overline{q^2}$ in equation (30) (or equation 32) is determined at the equivalent linear frequency $\Omega$ (or $\lambda$) which is in turn related to $\overline{q^2}$ through equation (26) (or equation 27). To determine the mean-square deflection, an iterative procedure is introduced. One can estimate the initial mean-square deflection $\overline{q_o^2}$ using linear frequency $\omega_o$ through equation (30) as

$$\overline{q_o^2} = \frac{\pi S(\omega_o)}{4m^2 \zeta \omega_o^3} \tag{34}$$

This initial estimate of $\overline{q_o^2}$ is simply the mean-square response based on linear theory. This initial estimate of $\overline{q_o^2}$ can now be used to obtain refined estimate

of $\Omega_1$ through equation (26), $\Omega_1^2 = \omega_o^2 + 3\beta \overline{q_o^2}$, then $\overline{q_1^2}$ is obtained through equation (30) as

$$\overline{q_1^2} = \frac{\pi S(\Omega_1)}{4m^2 \zeta \omega_o \Omega_1^2} \tag{35}$$

As the iterative process converges on the n-th cycle, the relation

$$\overline{q_n^2} = \frac{\pi S(\Omega_n)}{4m^2 \zeta \omega_o \Omega_n^2} \simeq \overline{q_{n-1}^2} \tag{36}$$

becomes satisfied. In the numerical results presented in the following section, convergence is considered achieved whenever the difference of the RMS displacements satisfied the relation

$$\left| \frac{\sqrt{\overline{q_n^2}} - \sqrt{\overline{q_{n-1}^2}}}{\sqrt{\overline{q_n^2}}} \right| \leq 10^{-3} \tag{37}$$

### Stress Response

Once the RMS displacement is determined, the bending stresses on the surface of the panel can be determined from

$$\sigma_{xb} = -\frac{6D}{h^2} (w,_{xx} + \nu w,_{yy})$$

$$\sigma_{yb} = -\frac{6D}{h^2} (w,_{yy} + \nu w,_{xx}) \tag{38}$$

From equations (3) and (38), and using equations (4), (6), (7) and (10), the expressions for the nondimensional stresses on the surface of a simply supported panel with immovable edges are given by

$$\frac{\sigma_x b^2}{Eh^2} = (\sigma_{xb} + \sigma_{xm}) \frac{b^2}{Eh^2} = [\frac{\pi^2}{2(1-\nu^2)}(\frac{1}{r^2} + \nu) \cos \frac{\pi x}{a} \cos \frac{\pi y}{b}] q$$

$$+ (\frac{\pi^2}{8r^2} \cos \frac{2\pi y}{b}) q^2 + [\frac{\pi^2 (1 + \nu r^2)}{8r^2 (1-\nu^2)}] q^2$$

$$\frac{\sigma_y b^2}{Eh^2} = (\sigma_{yb} + \sigma_{ym}) \frac{b^2}{Eh^2} = [\frac{\pi^2}{2(1-\nu^2)} (1 + \frac{\nu}{r^2}) \cos \frac{\pi x}{a} \cos \frac{\pi y}{b}] q$$

$$+ (\frac{\pi^2}{8} \cos \frac{2\pi x}{a}) q^2 + [\frac{\pi^2(r^2+\nu)}{8r^2(1-\nu^2)}] q^2 \qquad (39)$$

For movable inplane edges, the last term in equation (39) vanishes. Similarly, from equations (3) and (38), and using equations (7), (15), (17), and (18), the expressions for the nondimensional tensile stresses on the surface of a clamped panel with immovable edges are

$$\frac{\sigma_x b^2}{Eh^2} = \frac{\pi^2}{2(1-\nu^2)} [\frac{1}{r^2} \cos Ax(1+\cos By) + \nu(1+\cos Ax) \cos By] q$$

$$+ \frac{\pi^2 r^2}{8}[\frac{1}{r^4} \cos By + \frac{2}{(1+r^2)^2} \cos Ax \cos By + \frac{1}{4r^4} \cos 2By$$

$$+ \frac{1}{(4+r^2)^2} \cos 2Ax \cos By + \frac{4}{(1+4r^2)^2} \cos Ax \cos 2By]q^2$$

$$+ [\frac{3\pi^2(1+\nu r^2)}{32r^2(1-\nu^2)}] q^2 \qquad (40)$$

$$\frac{\sigma_y b^2}{Eh^2} = \frac{\pi^2}{2(1-\nu^2)} [(1+\cos Ax) \cos By + \frac{\nu}{r^2} \cos Ax(1+\cos By)] q$$

$$+ \frac{\pi^2}{8} [\cos Ax + \frac{1}{4} \cos 2Ax + \frac{2}{(1+r^2)^2} \cos Ax \cos By$$

$$+ \frac{4}{(4+r^2)^2} \cos 2Ax \cos By + \frac{1}{(1+4r^2)^2} \cos Ax \cos 2By] q^2$$

$$+ [\frac{3\pi^2(r^2+\nu)}{32r^2(1-\nu^2)}] q^2$$

where $A = 2\pi/a$ and $B = 2\pi/b$. For movable edges, the last term in equation (40) vanishes.

Examining equations (39) and (40), a general expression is obtained for the stress at any point in the structure as

$$\sigma = c_1 q + c_2 q^2 \tag{41}$$

where $c_1$ and $c_2$ are constants. The constants can be determined from material properties, dimensions of the panel, and the location and direction at which the stress is to be measured. The mean-square stress is then related to the mean-square modal amplitude in a general expression as

$$\overline{\sigma^2} = c_1^2 \, \overline{q^2} + 3 \, c_2^2 \, (\overline{q^2})^2 \tag{42}$$

Once the mean-square deflection $\overline{q^2}$ is determined, equations (36) and (37), the mean-square stress can then be obtained from equation (42).

## RESULTS AND DISCUSSION

Because of the complications in analysis of the many coupled modes, only one-mode approximation is used in the formulation. The assumption for fundamental mode predominacy is admittedly overly simplified; the conditions under which this is a valid approximation remain to be investigated. However, a simple model sometimes helps to give basic understanding of the problem.

Using the present formulation, response of nonlinear rectangular panels with all edges simply supported and all edges clamped subjected to broadband random acoustic excitation are studied. Both immovable and movable inplane edges are considered. In the results presented, the spectral density function of the excitation pressure S(f) is considered flat within a certain region near the equivalent linear frequency f and a value of Poisson's ratio of 0.3 is used in all computations, unless otherwise mentioned. Mean-square amplitudes and mean-square nondimensional stresses for panels of various aspect ratios and damping ratios are determined and presented in graphical form. These graphs can be used as guides for preliminary design of aircraft panels. The maximum mean-square deflection can be reasonably obtained from these figures; however, multiple modes had to be considered for accurate determination of mean-square stresses. This has been demonstrated by Seide in reference 15 for a simple beam subjected to uniform pressure excitation and in reference 16 for large deflections of prestressed simply supported rectangular plates under static uniform pressure. Comparison with experiment is also given. It is demonstrated that the present formulation gives remarkable improvement in predicating RMS responses as compared with using the linear theory.

### Analytical Results

Figure 2 shows the maximum mean-square nondimensional deflection versus nondimensional spectral density parameter of acoustic pressure excitation for rectangular panels of aspect ratios $r = 1, 2,$ and $4$, and a damping ratio 0.02. It is clear from the figure that an increase of r will "close" the curve.

This occurs because as r increases, the panel becomes less stiff, and the mean-square deflection has to be finite. It can also be seen from the figure that the mean-square deflection of the movable inplane edges case is approximately twice as that of the immovable edges.

The maximum mean-square nondimensional stress (bending plus membrane stress, at the center of the panel and in the y-direction) is given in Figure 3 as a function of excitation spectral density parameter for simply supported rectangular panels of various aspect ratios and a damping factor 0.02. Results showed that the difference of maximum mean-square stresses between immovable and movable edges is small as compared with the difference of mean-square deflections between the two edge conditions.

Figure 4 shows the mean-square deflection versus forcing spectral density parameter for simply supported square panels of different damping ratios. The corresponding maximum mean-square stress (bending plus membrane stress, at the center of panel) is shown in Figure 5. As it can be seen from the figure that the precise determination of damping ratio from experiment is important, e.g., stress increases by 25-30 percent as $\zeta$ is decreased from 0.015 to 0.01 (for $S_f$ between 5000 to 20000).

Plots of the equivalent linear or nonlinear frequency parameter $\lambda^2$ versus mean-square modal amplitude for simply supported rectangular panels of aspect ratios r = 1, 2, and 4 are shown in Figure 6. The lowest value of $\lambda^2$ corresponds to the linear case.

In Figure 7, the mean-square deflection is given as a function of excitation spectral density parameter for rectangular panels of aspect ratios r = 1, 2, and 4 and a damping ratio 0.02. The maximum mean-square deflection of the clamped panels is somewhat much less than that of the simply supported. The corresponding maximum mean-square nondimensional stress (bending plus membrane stress, in the y-direction and at the center of the long edge) versus spectral density parameter is shown in Figure 8.

Figure 9 shows the mean-square modal amplitude versus spectral density parameter of excitation for a square panel of different damping ratios. In Figure 10, the equivalent linear frequency parameter is given as a function of mean-square deflection for clamped rectangular panels of aspect ratios r = 1, 2, and 4.

### Comparison with Experimental Results

The experimental measurements on skin-stringer panels exposed to random pressure loads reported in references 3 and 4 are used to demonstrate the improvement in predicting panel responses by using the present formulation. The structure was a skin-stringer, 3-bay panel as shown in Figure 11. The panels were constructed of 7075-T6 aluminum alloy. Details of the test facility, noise sources, test fixture, and test results are given in reference 3. The important properties of the panel are

| Length | $a = 68.58$ cm (27 in.) |
|---|---|
| Width between the rivet lines | $b = 16.84$ cm (6.63 in.) |
| Thickness | $h = 0.81$ mm (0.032 in.) |
| Damping ratio | $\zeta = 0.0227$ |
| Poisson's ratio | $\nu = 0.33$ |
| Young's modulus | $E = 66.19 \times 10^3$ MPa ($9.6 \times 10^6$ psi) |
| Weight density | $\rho = 7.164$ kg/m$^3$ (0.1 lb/in.$^3$) |

The tests were conducted with an overall sound pressure level (SPL) of 157 dB, with a range of $\pm$ 1.5 dB which corresponds to an average spectrum level of 125.26 dB (see Table IV of ref. 3 or Table 8 of ref. 17). The central bay of the 3-bay test panels is simulated by a flat rectangular plate. The linear frequencies for both simply supported (equation (14)) and clamped (equation (20)) support conditions are calculated and shown in Table 1. Test measurements and finite element solution are also given for comparison. Table 1 also shows the equivalent linear or nonlinear frequencies at overall SPL 157 dB.

<div align="center">Table 1.  Frequency Comparison</div>

|  | Natural frequency $f_o$ | Equivalent linear frequency $f_{157}$ |
|---|---|---|
| Simply supported  – Immovable edges | 71 | 321 |
| – Movable edges | 71 | 240 |
| Clamped – Immovable edges | 159 | 311 |
| – Movable edges | 159 | 264 |
| Finite element (ref. 4) | 155 | N/A |
| Experiment (ref. 3) | 126, 129 | N/A |

Frequency at high intensity noise level was not reported in reference 3. From the results shown in Table 1, it is clear that the central bay of the test panels did not respond to the acoustic excitation as though it were fully clamped on all four edges. This was also demonstrated in Figures 12 and 17 of reference 3 in the sense that the highest measured RMS strains did not occur at the center of the long edges. The central bay of the test panels actually behaved somewhat between fully simply supported and fully clamped support conditions.

The acoustic pressure spectral density S(f) is related to the spectrum level L as

$$S(f) = \begin{cases} 8.41 \times 10^{(L/10 - 18)} & \text{(psi)}^2/\text{Hz} \\ \\ 4 \times 10^{(L/10 - 8)} & \text{(dynes/cm}^2)^2/\text{Hz} \end{cases} \quad (47)$$

A spatially uniform white noise pressure loading with spectral density of $S(f) = 2.824 \times 10^{-5}$ (psi)$^2$/Hz (or nondimensional spectral density parameter $S_f = 5100$), which corresponds to an average spectrum level L = 125.26 dB, is used in the computations. The RMS stresses (equation (42)) at the center of the long edges for simply supported (equation (39)) and clamped (equation (40)) boundary conditions are calculated and given in Table 2.

Table 2. Stress Comparison

(RMS stress, kpsi at overall SPL 157 dB)

| | $\sqrt{\overline{\sigma_x^2}}$ | | $\sqrt{\overline{\sigma_y^2}}$ | |
| --- | --- | --- | --- | --- |
| | Linear Theory | Nonlinear Theory | Linear Theory | Nonlinear Theory |
| Simply-Supported | 0.0 | 0.58(Im.) 0.17(Movable) | 0.0 | 3.28(Im.) 2.74(Movable) |
| Clamped | 2.17 | 1.12(Im.) 1.32(Movable) | 6.57 | 3.84(Im.) 4.24(Movable) |
| Finite Element (ref. 4) | 2.4 | NA | 7.7 | NA |
| Experiment (refs. 3, 4) | | | | |
| Panel A | | 0.63 | | 2.2 |
| Panel B | | 0.94 | | 2.9 |
| Panel C | | 0.78 | | 2.5 |
| Panel D | | 1.1 | | - |
| Panel E | | 0.84 | | 2.2 |
| Average A-E | | 0.87 | | 2.5 |

Table 3 shows the RMS deflections using the present formulation. The measured and finite element RMS stresses and RMS deflections in reference 4 are also given in the tables for comparison. It demonstrates that a better correlation between theory and experiment can be achieved when large deflection geometrical nonlinearity effect is included in the formulation.

Table 3. Deflection Comparison

$$\sqrt{(w_{max}/h)^2}$$

| | Linear Theory | Nonlinear Theory |
|---|---|---|
| Simply Supported | 8.0 | 1.8 (Immovable) |
| | | 2.4 (Movable) |
| Clamped | 2.7 | 1.4 (Immovable) |
| | | 1.6 (Movable) |
| Finite Element (ref. 4) | 3.1 | NA |
| Measured (refs. 3, 4) | - | 2.0 |

CONCLUDING REMARKS

An analytical method for predicating response of rectangular nonlinear structural panels subjected to broadband random acoustic excitation is presented. The formulation is based on the Karman-Herrmann large deflection plate equations, a single-mode Galerkin approximation, the equivalent linearization method, and an iterative procedure. Both simply supported and clamped support conditions with immovable or movable inplane edges are considered. Panel mean-square deflection, maximum mean-square stress, and equivalent linear frequency at given excitation pressure spectral density can be determined, and they are presented in graphical form. These graphs can be used as guides for preliminary design of aircraft panels under high noise environment. Results obtained agree well with the experiment. It is suggested that further research be carried out with special attention to employ multiple modes in the formulation for accurate determination of mean-square stresses, and additional test data on simple panels are needed for an adequate quantitative comparison.

REFERENCES

1. Rudder, F. F., Jr. and Plumblee, H. E., Jr., "Sonic Fatigue Design Guide for Military Aircraft", AFFDL-TR-74-112, W-PAFB, OH, May 1975.

2. Fitch, G. E. et al, "Establishment of the Approach to and Development of Interim Design Criteria for Sonic Fatigue", ASD-TDR-62-26, W-PAFB, OH, June 1962.

3. Van der Heyde, R. C. W. and Smith, D. L., "Sonic Fatigue Resistance of Skin-Stringer Panels", AFFDL-TM-75-149-FYA, W-PAFB, OH, April 1974.

4.  Jacobs, L. D. and Lagerquist, D. R., "Finite Element Analysis of Complex Panel to Random Loads," AFFDL-TR-68-44, W-PAFB, OH, October 1968.

5.  Jacobson, M. J., "Advanced Composite Joints: Design and Acoustic Fatigue Characteristics," AFFDL-TR-71-126, W-PAFB, OH, April 1972.

6.  Jacobson, M. J., "Sonic Fatigue Design Data for Bonded Aluminum Aircraft Structures," AFFDL-TR-77-45, W-PAFB, OH, June 1977.

7.  Mei, C., "Large Amplitude Response of Complex Structures Due to High Intensity Noise," AFFDL-TR-79-3028, W-PAFB, OH, April 1979.

8.  Chu, H. N. and Herrmann, G., "Influence of Large Amplitudes on Free Flexural Vibrations of Rectangular Elastic Plates," J. of Applied Mechanics, Vol. 23, December 1956, pp. 532-540.

9.  Caughey, T. K., "Equivalent Linearization Techniques," JASA, Vol. 35, November 1963, pp. 1706-1711.

10. Caughey, T. K., "Nonlinear Theory of Random Vibrations," in Advances in Applied Mechanics, Vol. 11, Yih, C. S., ed., Academic Press, 1971, pp. 209-253.

11. Spanos, P. T. D. and Iwan, W. D., "On the Existence and Uniqueness of Solutions Generated by Equivalent Linearization," Int. J. of Non-Linear Mechanics, Vol. 13, 1978, pp. 71-78.

12. Timoshenko, S. and Woinowsky-Krieger, S., Theory of Plates and Shells, McGraw-Hill, 1959, pp. 415-428.

13. Lin, Y. K., "Response of a Nonlinear Flat Panel to Periodic and Randomly-Varying Loadings," J. Aero. Sci., September 1962, pp. 1029-1033, p. 1066.

14. Yamaki, N., "Influence of Large Amplitudes on Flexural Vibrations of Elastic Plates," Z. Angew. Math. Mech., Vol. 41, 1961, pp. 501-510.

15. Seide, P., "Nonlinear Stresses and Deflections of Beams Subjected to Random Time Dependent Uniform Pressure," ASME Paper No. 75-DET-23, 1975.

16. Seide, P., "Large Deflections of Prestressed Simply Supported Rectangular Plates under Uniform Pressure," Int. J. Non-Linear Mechanics, Vol. 13, 1978, pp. 145-156.

17. Van der Heyde, R. C. W. and Wolfe, N. D., "Comparison of the Sonic Fatigue Characteristics of Four Structural Designs," AFFDL-TR-76-66, W-PAFB, OH, September 1976.
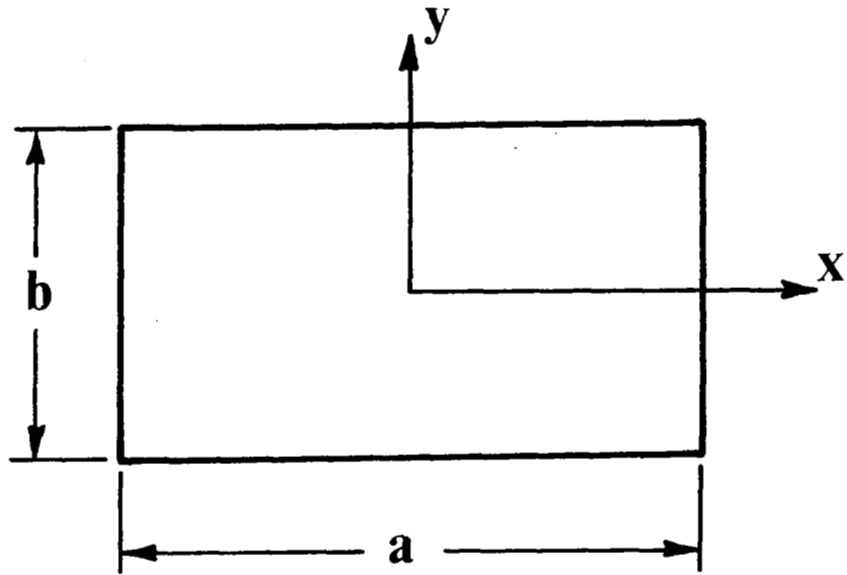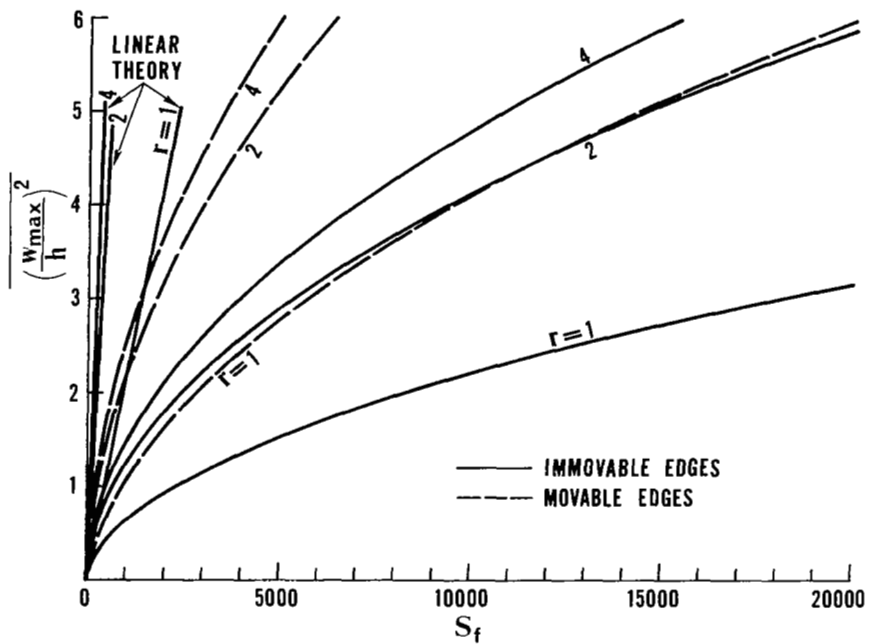
Figure 1. Geometry and coordinates.



Figure 2. Mean-square deflection versus spectral density parameter of excitation for simply supported panels, $\zeta = 0.02$.
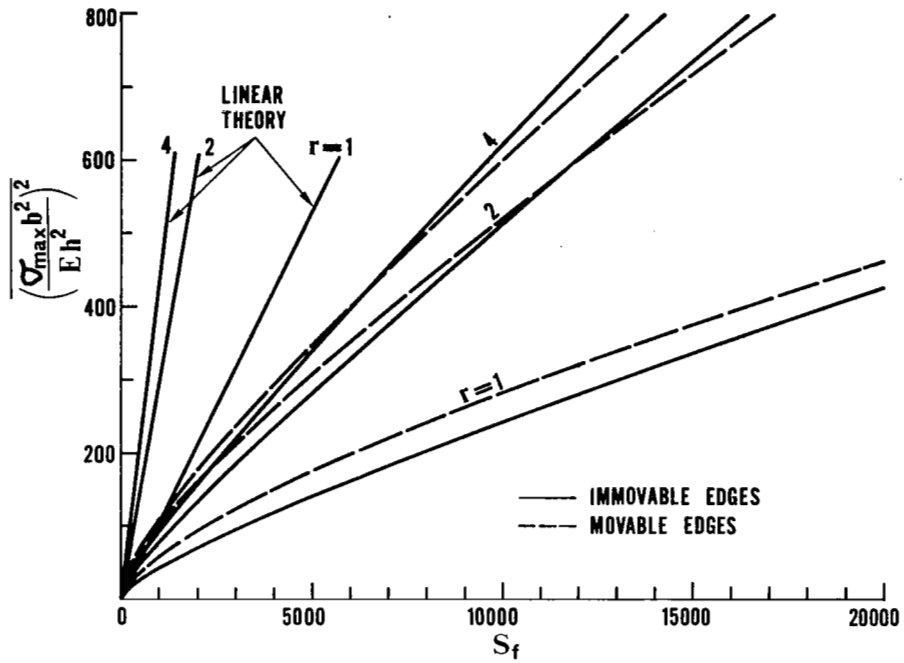
Figure 3. Maximum mean-square stress versus spectral
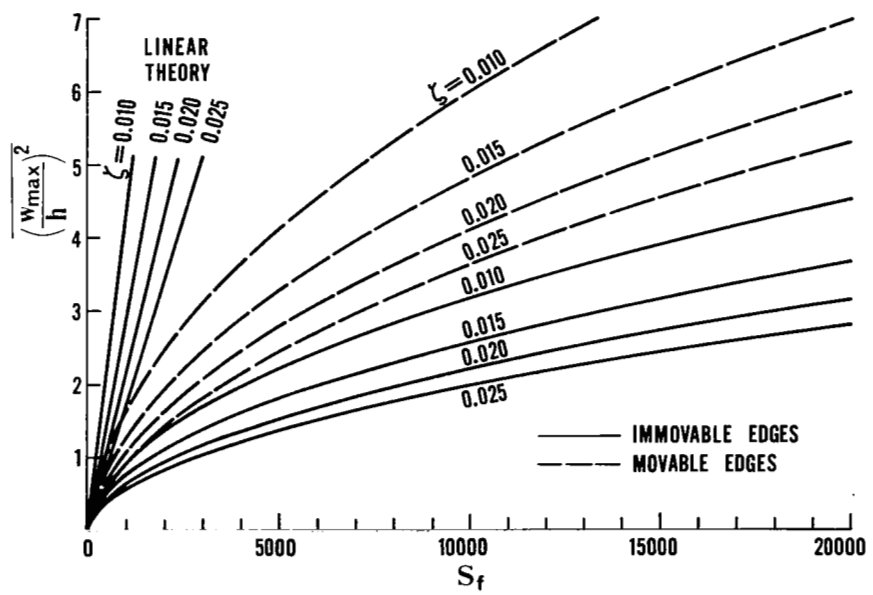density parameter of excitation for simply
supported panels, $\zeta = 0.02$.



Figure 4. Effect of damping on mean-square deflection for a
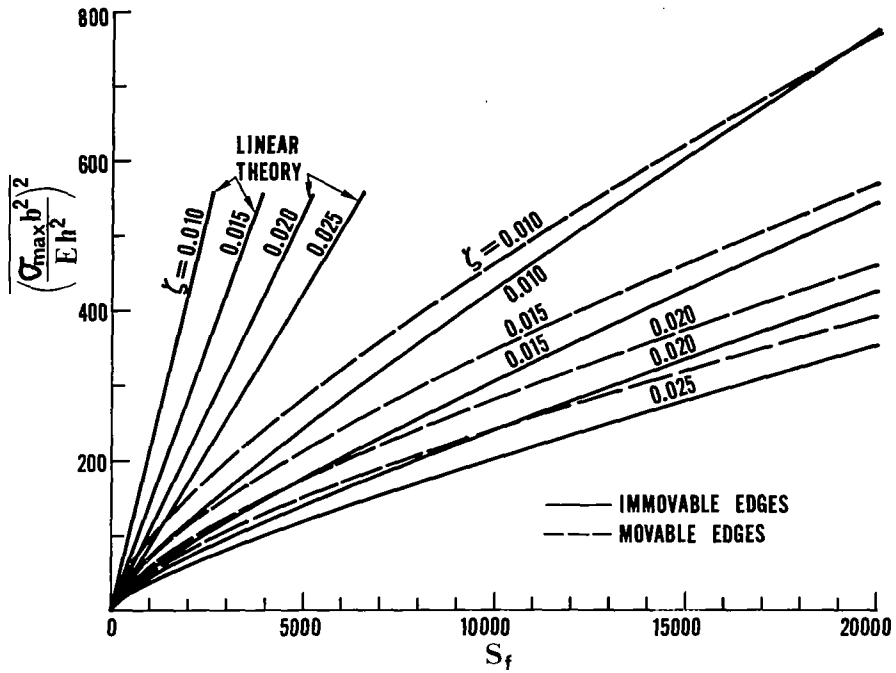simply supported square panel.

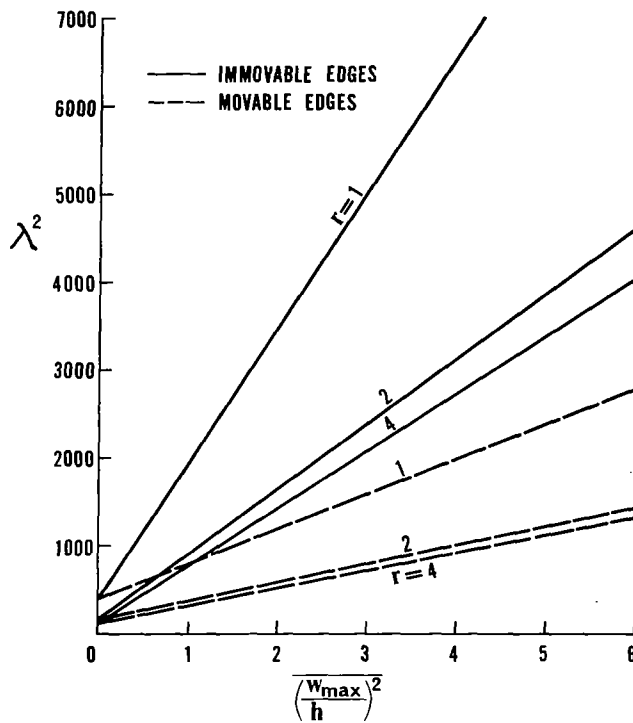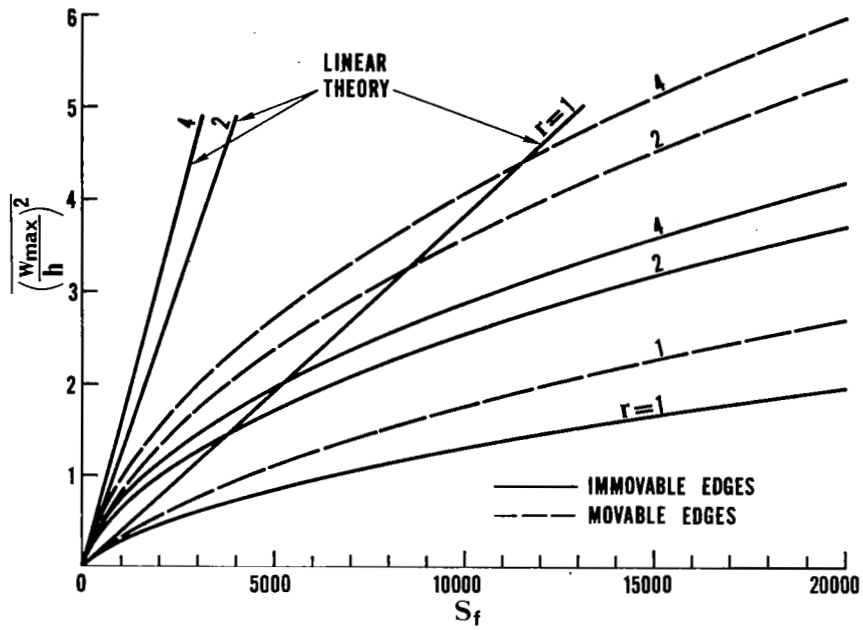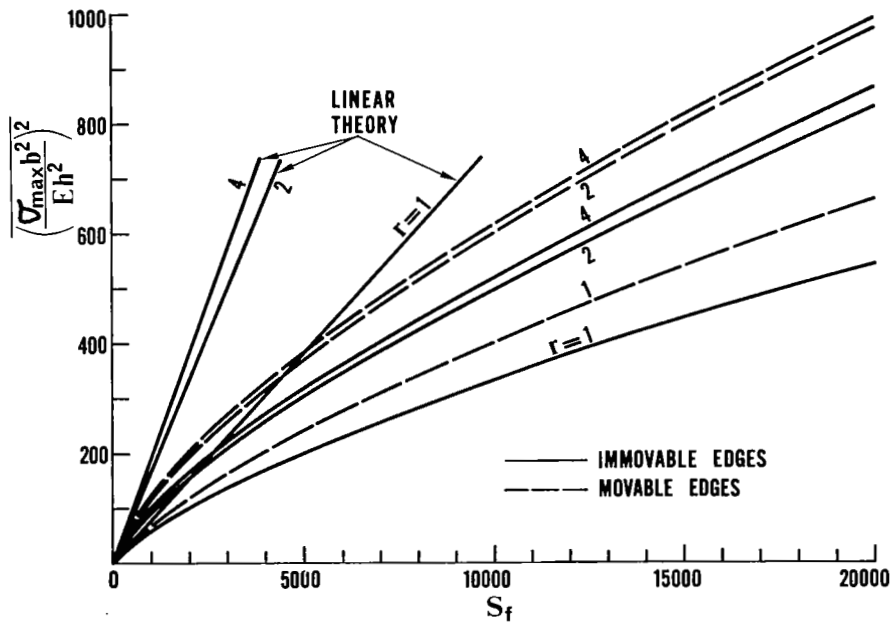Figure 5. Effects of damping on maximum mean-square
stress for a simply supported square panel.



Figure 6. Frequency parameter versus mean-square
deflection for simply supported panels.

Figure 7.   Mean-square deflection versus spectral density
parameter of excitation for clamped panels,
$\zeta = 0.02$.



Figure 8.   Maximum mean-square stress versus spectral density
parameter of excitation for clamped panels,
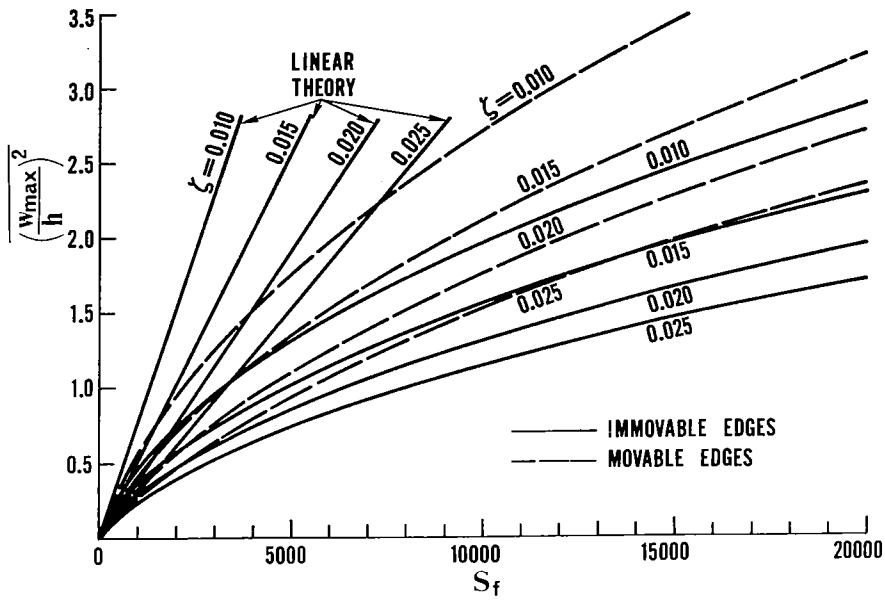$\zeta = 0.02$.

Figure 9.   Effects of damping on mean-square deflection
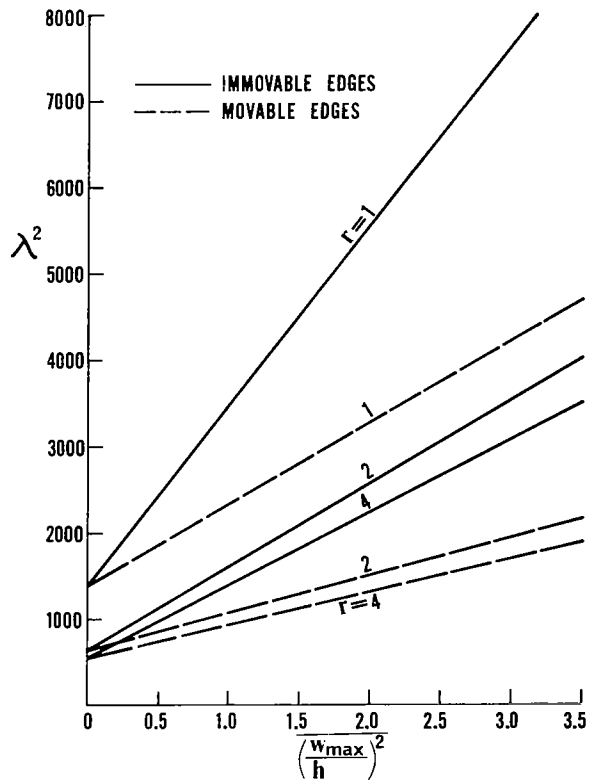            for a clamped square panel.



Figure 10.   Frequency parameter versus mean-square
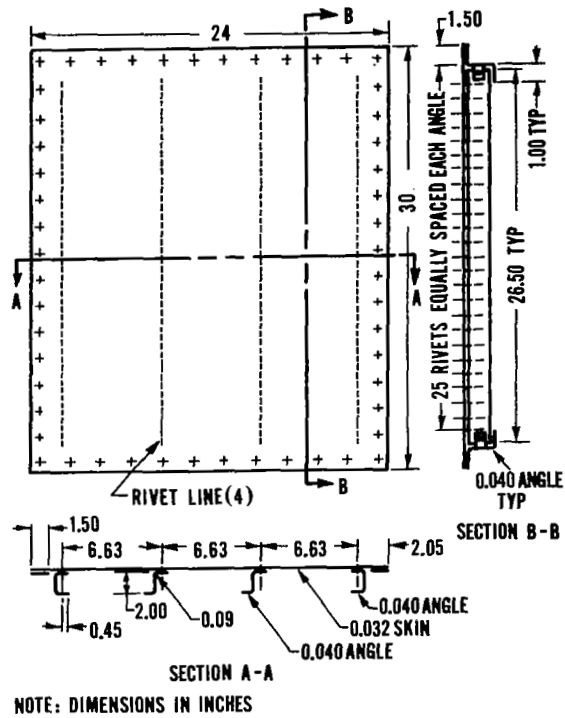             deflection for clamped panels.

Figure 11. Skin-stringer panel (after Van der Heyde and Smith, ref. 3).